Pages: 88-98 / Vol. 18 / Issue 2 / Summer-Fall 2025

Journal of Aerospace Science and Technology

Journal Homepage: https://jast.ias.ir

Original Research Article

Quasi-static and Dynamic Analysis of a 12U Cubesat Under flight-phase Environmental Loads

Amir Reza Haddadi[1], S. Mohammad Navid Ghoreishi[2*], Yaser Sedigh[3], and Hossien Shabani[4]

1, 4. Department of Mechanical Engineering, Sharif University of Technology, Tehran, Iran
2. Satellite Research Institute, Iranian Space Research Center, Tehran, Iran
3. Department of Mechanical Engineering, K.N. Toosi University of Technology, Tehran, Iran

TICLE INFO

Received: 29 August 2024
Revised: 02 January 2025
Accepted: 04 January 2025
Available online: 07 May 2025

KEYWORDS:

CubeSat
Dynamic analysis
Finite element method
Environmental loads

DOI: 10.22034/jast.2025.475926.1207

ABSTRACT

CubeSats are a class of nanosatellites that, despite being small, are able to perform important space missions without the need for large and complicated satellites. Since during the operational life of the satellite, especially during the launch phase, various quasi-static and dynamic loads are applied to the satellites, therefore, the strength and dynamic analyses of the satellite structure, as the main element to tolerate external loads, are of great importance. In this paper, the mechanical design and full finite element analysis of the structure of a 12U remote-sensing CubeSat, including modal, random vibrations, sinusoidal vibrations, and quasi-static analysis, are performed. First, the design process of the presented 12U CubeSat, which fulfills the requirements of CubeSats, is expressed. In the design of the structure, a middle plate is used to increase the stiffness and natural frequencies. Second, Ansys Software performs the finite element analysis of the satellite according to the ECSS standard. The numerical results show that the designed structure meets all requirements of the launcher, including stiffness and frequency requirements while sustaining the static and dynamic loads during the launch phase.

1 INTRODUCTION

In recent years, with the advent of microsatellites and nanosatellites, space missions have become possible with less cost and time. CubeSats, introduced in 1999 as a collaborative effort by California Polytechnic State University and Stanford University, revolutionized the satellite industry with their compact, multidisciplinary, and standardized design. Initially developed as an educational tool to provide students with hands-on experience in space technology. Their affordability, rapid development cycles, and adaptability have made CubeSats instrumental in advancing research, Earth observation, communication, and technology demonstrations. Over the past two decades, they

* Corresponding Author's Email: smn.ghoreishi@isrc.ac.ir

Print ISSN:1735-2134 Online ISSN: 2345-3648

have transitioned from academic projects to critical components of commercial and scientific satellite missions, fostering innovation and accessibility in space exploration.

CubeSats are available in different sizes and masses, ranging from 1U to 12U and recently up to 27U. Every 1U measures 100mm×100mm×100mm and with a maximum mass of 1.33 kg; while a 12U cubesat measures 226mm×226mm×340mm and with a maximum mass of 24kg, based on California Polytechnic State University (CalPoly) [1]. California Polytechnic State University (CalPoly) and Stanford University's Space System Development Laboratory published a standard including the CubeSat's program and fundamental requirements, accompanied by guidelines for design progress.

In all space missions consisting of CubeSats, the structure is one of the important subsystems. Generally, the duty of a satellite structure is to tolerate all external mechanical and thermal loads in each phase and provide a suitable space for the operation of all modules and subsystems. In addition, the structure attaches the satellite to the launch vehicle [2].

So far, there have been many works investigating static and dynamic analysis of CubeSats. Burger et al. [3] analyzed static and modal analysis of the PCB board and its structure under loads produced in the launch phase numerically. Arroyave et al. [4] established a protocol for designing of cubesats and satisfying all of the structural and requirements of a given mission. Moreover, they performed static, modal, random, and harmonic analyses of a specific 1U cubesat under launch-phase loads. Barsoum et al. [5] investigated static, modal, random vibration, and fatigue life analysis on a student-designed 1U cubesat. Alhammadi et al. [6] conducted analytical and experimental static, modal, and random vibration analysis for a 1U cubesat. Reyes et al. [7] investigated modal, harmonic, and random vibration of a 1U cubesat using the finite element method and verified with analytical models. Ampatzoglou et al. [8] proposed a full-body composite 1U cubesat and compared its stiffness and fundamental frequency with an aluminum one. The results showed that using composite side panels can offer similar levels of performance in terms of stiffness while reducing mass by approximately 40%.

Chao and Vo [9] performed Dynamic analysis, including modal, harmonic, and random vibrations on a 3U cubesat numerically. A comprehensive expression of the design, modeling, and analysis of a 3U cubesat was conducted by Almazrouei et al. [10]. Ampatzoglou and Kostopoulos [2] presented design optimization, development, analysis, and verification of a 2U cubesat with composite body side panels using finite element method (FEM) and experimental tests. The results showed a 30% reduction in the total mass of the structure. Cihan et al. [11] proposed a new rack-based 3U cubesat and analyzed quasi-static, modal, and random vibration. This CubeSat allows the engineers to experiment with the design during the prototyping phase. Lima et al. [12] designed and analyzed a 2U cubesat numerically and assessed the presence of PBC boards on the vibrational characteristics of the satellite. Guvenc et al. [13] conducted quasi-static, dynamic, heat transfer, and thermal stresses induced by heat transfer in the launch phase on a 3U cubesat using the finite element method. Aswin et al. [14] performed static, modal, and heat flow analysis of a 3U cubesat. Guentchev et al. [15] investigated static, modal, random, Shock, and thermal analysis on a 12U cubesat using the finite element method. Configuration optimization of interior modules was conducted by Abbasy et al. [16] and Hekmatfar et al. [17, 18].

Considering the high range of quasi-static and vibrational loads caused by the launcher in the launch phase and the sensitivity of larger CubeSats (i.e., 12U and larger) to vibrations, analysis of the integrity and robustness of the main structure, including subsystems under the mentioned loads, will be very important. In this work, the design and dynamic analysis of the 12U cubesat were performed using commercial finite element software, ANSYS 2020. In the first section, the design procedure, including requirements and constraints, is expressed, and the accommodation of subsystems in the satellite is presented. In the 2nd section, stress and deformation analysis of the satellite under quasi-static loads is investigated, and in the 3rd section, dynamic analysis, including modal, harmonic, and random vibration behavior of the satellite under dynamic loads, is performed. All of the designs and analysis requirements are according to ECSS standards.

2 DESIGN METHODOLOGY

In the design of the structure of satellites, in addition to determining the external and internal positioning of the equipment and subsystems, achieving sufficient strength and stiffness along with appropriate frequency conditions of the launcher is

of great importance. In general, there are fundamental factors and procedures in the positioning of equipment, based on which the overall configuration of the satellite can be determined.

The process required for designing, analyzing, and testing the structure of a satellite is shown in Fig. 1. According to Fig. 1, for designing the structure of a satellite, firstly, the type and characteristics of the launcher must be determined. Then, the limitations of subsystems and flight equipment are considered based on it in order to determine the initial configuration of the satellite. The primary structure should be designed in such a way that it can withstand the mechanical loads induced by the launcher. In the next step, a finite element model of the structure of the satellite is produced with the help of commercial finite element software such as ABAQUS, NASTRAN, or ANSYS. In the following, using the finite element model he developed, all static and dynamic analyses can be simulated. If, after analysis, stress limits are not within the safe range or the natural frequencies are so close to the natural frequencies of the launcher, the structure of the satellite must be redesigned from the beginning.

3 CONSTRAINTS AND REQUIREMENTS OF THE DESIGN OF CUBESATS

There are constraints and requirements for the design and configuration of equipment in cubesats that should be considered in order to reach to an optimal design.

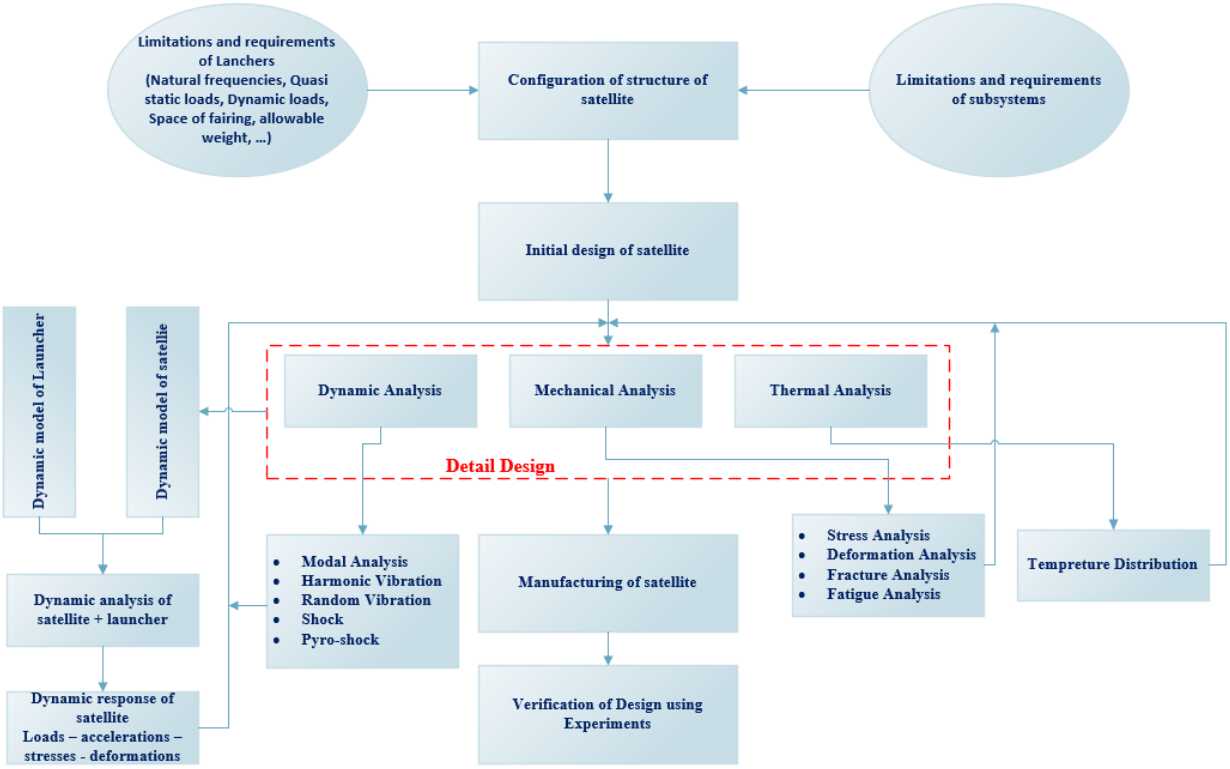

Fig. 1. Algorithm of design, analysis, and test of satellites

- **Stiffness and strength**

The structure of the satellite should have enough stiffness in order to withstand external loads induced by the launcher.

- **Space and volume**

The configuration of equipment and the amount of volume of the satellite should be enough to install and prevent interference with each other. Moreover, configuration and positioning should be performed in such a way that has the least occupied volume and mass. The dimensions of the structure under study are according to CubeSat standards, i.e., CalPoly [1], shown in Fig. 2. Based on the CalPoly standard, the dimensions and maximum weight of a 12U CubeSat are

226mm×226mm×340mm, and the maximum weight up to 24 kg.

- **Accessibility**

The position and orientation of assembled equipment should be in such a way that provides accessibility to every module during the assembling, testing, and maintenance phases.

- **Inertial and mass characteristics**

The equipment should be configured in such a way that the mass and inertial characteristics of the satellite are within the allowable range. According to CalPoly, the maximum allowable moment of inertia of 12U cubesat is within 4.5 cm.

- **Manufacturing**

The simplicity of manufacturing, use of available materials, cost, and final weight of a satellite are among the most important design parameters that should be considered.

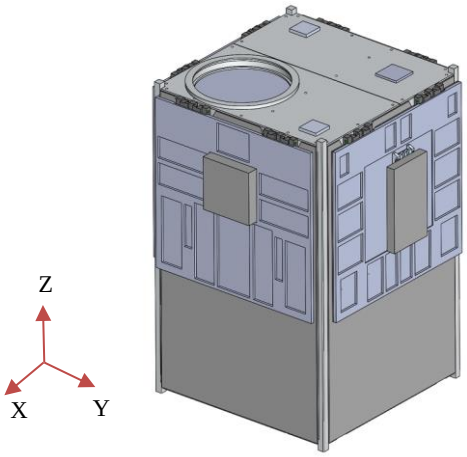

Fig. 2. The structure of the presented 12U cubesat and the coordinate system

4 STRUCTURE UNDER STUDY

In this work, the structure of the satellite under study is a 12U cubesat class satellite with a sensing mission, according to the mentioned requirements and considerations, the equipment and subsystems have been assembled in this 12U cubesat, depicted in Fig. 2.

The body side plates of the structure have up to 1.5mm thickness and are designed in such a way that both it is possible to access inside the structure and also satisfy the requirements of all other subsystems. The structure shown in Fig. 4 is the final design of the structure.

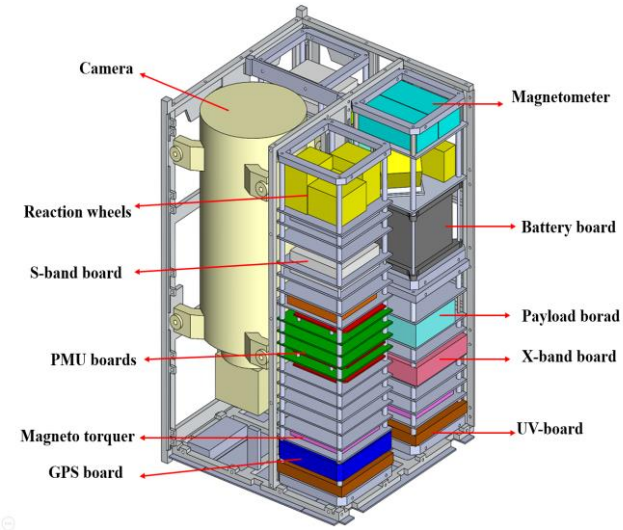

Fig. 3. Configuration of equipment in a 12U cubesat with simplified modules

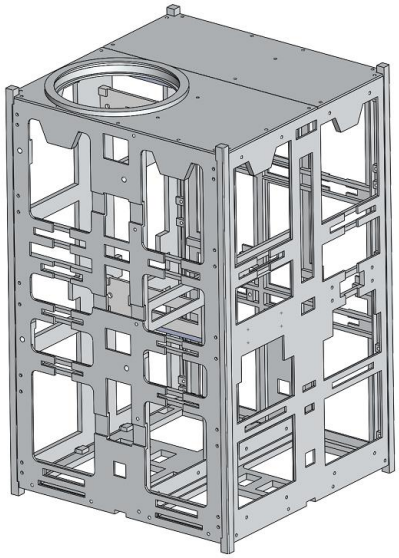

Fig. 4. Primary structure of the presented 12U CubeSat

5 MATERIAL

The material used in the primary structure of the 12U cubesat is aluminum alloy 6061-T6 because of its suitable stiffness-to-mass ratio, which has optimized properties for vibration environments. Aluminum ally 6061-T6 is one of the most widely used materials in the space industry, referred to in many works (i.e., [2,19-21]). The mechanical properties of Aluminum alloy 6061-T6 are illustrated in Table 1.

Also, PCBs (Printed Circuit Board) are simplified with no components (i.e., connectors,

capacitors, etc.) since these components do not have much mass, while complex geometries increase computational cost significantly. The PCB boards are made of FR-4, a polymer-based material. The Mechanical properties of FR-4 are listed in Table 2.

Table 1. Mechanical properties of Aluminum alloy 6061-T6

Mechanical property	Value
Density (kg/m^3)	2750
Young's modulus (GPa)	69
Poisson's ratio	0.33
Shear modulus (GPa)	25.94

Table 2. Mechanical properties of FR-4

Mechanical property	Value
Density (kg/m^3)	1840
Young's modulus, X-direction (GPa)	20.4
Young's modulus, Y- direction (GPa)	18.4
Young's modulus, Z- direction (GPa)	15
Poisson's ratio, XY-plane	0.11
Poisson's ratio, YZ-plane	0.09
Poisson's ratio, XZ-plane	0.14
Shear modulus, XY-plane (GPa)	9.2
Shear modulus, YZ-plane (GPa)	8.4
Shear modulus, XZ-plane (GPa)	6.6

In this work, to reduce the computational cost, all modules and equipment have been substituted with their equivalent mass in such a way that the actual mass of that module or equipment is divided by the modeled geometry volume in the SOLIDWORKS software to obtain equivalent density. Then, the obtained equivalent densities are entered into the FEM software (ANSYS WORKBECH) as density. The actual mass of each module and equipment is depicted in Table 3. Furthermore, after positioning the modules within the satellite, the satellite's center of mass deviates by +1.2mm along the x-axis, -0.8 mm along the y-axis, and +1.1mm along the z-axis from its geometric center.

Table 3. Mass and inertial characteristics of the 12U CubeSat satellite and its equipment

Subsystem	Equipment	Value (kg)
ADCS	Gyro	0.200
	Star tracker	0.400
	Magnetometer	0.360
	Reaction wheel	0.520
	Magneto torquer	0.400
	GPS	0.230
Payload	Camera	4.200
	Receiver	0.900
Power	Battery board	0.500
	Battery pack	1.050
TT&C	S-band board	0.350
	X-band board	0.360
	UV-board	0.357
OBC	OBC boards	0.496
Structure	Structure	3.186
PRP	Thruster	2.000
	Total mass (kg)	14.876

6 ANALYSIS PROCEDURE

During launch, static and dynamic loads induced by the launcher are applied to the CubeSat satellite through the interface ring. As mentioned earlier, the structure should sustain these loads and keep satellite integrity. Various types of loads induced by the launcher are as follows [22]:

- Quasi-static induced
- Random vibration
- Harmonic vibration
- Shock

6.1 Quasi-static loads

The loads induced by the propulsion of the launcher are responsible for posing nearly constant loads along the axis of the launcher. These loads have been simulated in a quasi-static way in all three directions in g (gravity acceleration). According to the data of the launcher [23], the profile of longitudinal static acceleration of the launcher has been depicted in Fig. 5. Moreover, the limit levels of quasi-static loads, to be taken into account for design and dimensioning of the spacecraft primary structure, are listed in Table 5.

As seen in Table 4, the most amount of quasi-static load is applied during the first stage of flight and is 5g, whereas in the qualification level, this value becomes 10g by increasing +6 dB.

6.2 Modal analysis

In the launching phase, due to the existence of dynamic and quasi-static loads with high amplitudes, modal analysis of the satellite and extracting modal characteristics (including natural frequencies, mode shapes, and effective masses) are of most importance. In order to prevent the resonance phenomenon in a satellite, the design of the satellite should be such that the longitudinal and lateral natural frequencies of the satellite are more than those of the launcher so as not to create any coupling between the satellite's and the launcher's modes. Frequency requirements announced by the launcher for satellite design are presented in Table 5.

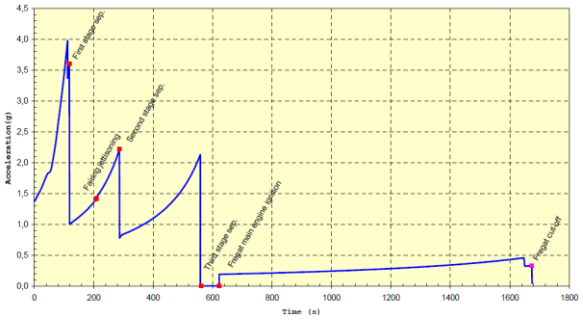

Fig. 5. Typical longitudinal static acceleration of the launcher

Table 4. Quasi-static loads induced by the Soyuz launcher during various phases [23]

phase	Design limit load (g) (+ = tension; - = compression)	
	Max lateral load	Max longitudinal load
Ground Transportation	±0.3	-1.3 to -0.7
Lift-off	±1.8	-1.6 to -0.4
Flight with maximum dynamic pressure	±1.1	-2.8 to -2.0
1st stage flight with maximal acceleration	±0.9	-5.0 to -3.6
Separation between 1st and 2nd stages	±1.1	-4.3 to -0.6
2nd stage flight	±1.2	-4.0 to -0.6
Separation between 2nd and 3rd stage	±0.8	-3.3 to +1.3
Beginning of the 3rd stage flight	±0.8	-2.9 to +0.9
3rd stage engine cutoff	±0.4	-4.0 to +1.8

Table 5. Frequency requirements by the launcher

Direction of the launcher	Value (in Hz)
Longitudinal (X)	65
Lateral (Y, Z)	25

6.3 Random vibrations

Random vibrations are mainly induced by engines, aerodynamic and acoustic phenomena, and transmitted through the connecting rig from the engine to the structure. The profile of random vibrations induced by the launcher is shown in Fig. 6 and Table 6 [23].

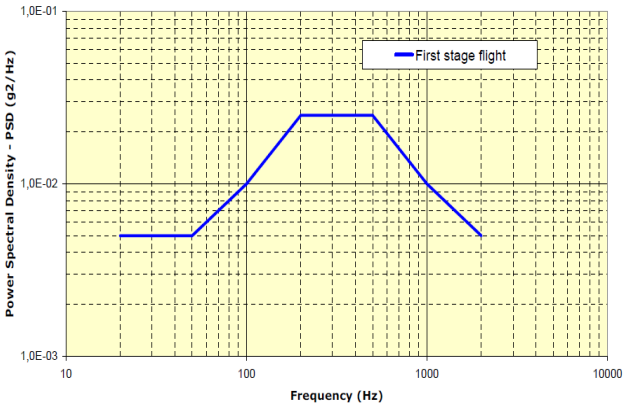

Fig. 6. Typical longitudinal Random Vibration of the launcher

Table 6. Random vibration induced by the Soyuz launcher during various phases [23]

Frequency (Hz)	Power spectral density (PSD) ($\times 10^{-3}$ g^2/Hz)		
	1st stage Grms = 4.94g	2nd and 3rd stage Grms = 3.31g	Fregat flight Grms = 1.63g
20-50	5.0	2.5	2.0
50-100	5 to 10.0	2.5 to 5	2.0
100-200	10.0 to 25.0	5.0 to 10.0	2.0
200-500	25.0	10.0	2.0
500-1000	25.0 to 10.0	10.0 to 5.0	2.0 to 1.0
1000-2000	10.0 to 5.0	5.0 to 2.0	1.0

In this work, all loads are carried out at the qualification level due to the ECSS standard. So, the

amplitude of the random vibration profile is increased by +6 dB.

6.4 Harmonic vibrations

Low-frequency harmonic vibrations are usually created by the interaction between the launcher mode shapes and applied loads during different phases of flight. The profile of harmonic loads of the launcher along longitudinal and lateral directions is shown in Fig. 7 and Table 7. All loads are applied at the qualification level due to the ECSS standard. So, the amplitude of the harmonic vibration profile is increased by 6 dB.

Table 7. Harmonic vibration induced by the launcher [23]

Frequency (Hz)	Amplitude (g)	
	Lateral	Longitudinal
1-5	0.4	0.4
5-10	0.6	0.5
10-20	0.6	0.8
20-30	0.4	0.8
30-40	0.4	0.5
40-60	0.3	0.5
60-100	0.3	0.3

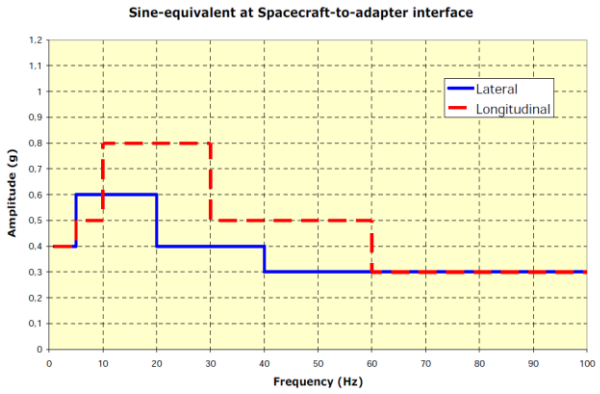

Fig. 7. Typical profile of longitudinal and lateral harmonic vibration of launcher [23]

7 FINITE ELEMENT ANALYSIS

To investigate the compliance of the satellite design with the launcher's requirements, a simplified model of the satellite has been performed, including primary and secondary structures as well as important components. In order to decrease computational costs, components with complex geometry are modeled as remote masses only (Fig. 8). To mesh the model, 106607 elements (97261 Hexagonal and 9346 tetrahedron elements) have been used, as shown in Fig. 9. The satellite is fixed at the external surfaces of the rails.

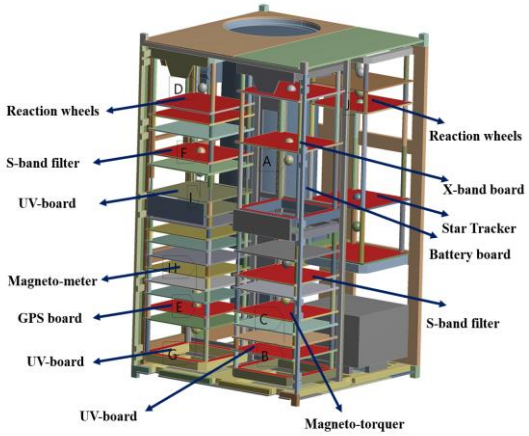

Fig. 8. Substituting lumped masses instead of the true geometries of components.

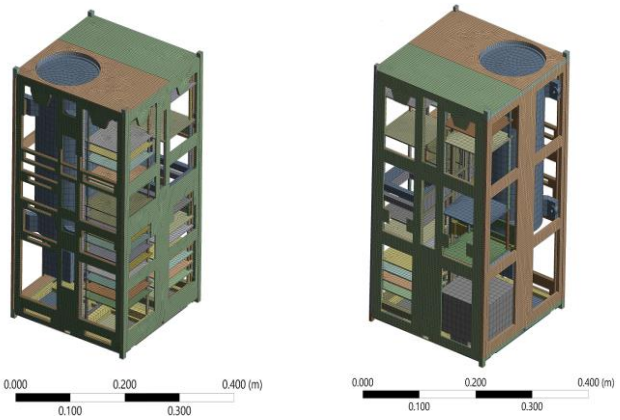

Fig. 9. Finite element model of 12U cubesat.

Resultes and Discussion

In modal analysis, the natural frequencies in the range of 0 to 2000 Hz are obtained. The first natural frequency of the satellites is 118.05 Hz along the axial direction, which is far enough away from the frequency of the launcher, with 65 Hz along the axial and 25 Hz along the transverse directions. The four mode shapes of the satellite are shown in Fig. 10, related to stacks 1 and 3 due to the long length and existence of heavy modules, respectively. Also, in Table 8, the first ten natural frequencies are presented.

In Figs. 11 and 12, the Von-Mises stress and deformations along x-, y-, and z-directions are illustrated. Maximum Von-Mises stress induced by quasi-static accelerations is equal to 61.07 MPa in the rod of stack 3, containing star sensors and battery board. Since the yield strength of Al 6061 is 450 MPa, the safety factor of the structure is equal to 7.36, which is a suitable amount. On the other hand, the deflections along x-, y-, and z-directions are 0.22

mm, 0.36 mm, and 0.01 mm, respectively. Because the maximum allowable deflection of the structure is 1.0 mm, therefore, the maximum deflection that occurred along the longitudinal direction is less than the allowable one.

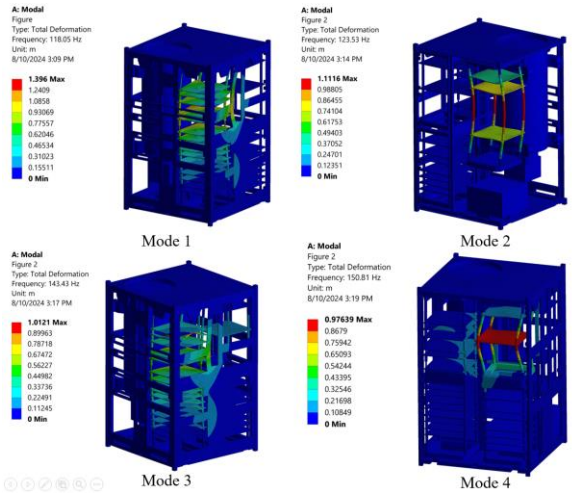

Fig. 10. The first four vibrational mode shapes

Table 8. Natural frequencies of a satellite

Mode number	Value (in Hz)
1	118.1
2	123.5
3	143.4
4	150.8
5	162.2
6	166.8
7	194.2
8	199.6
9	208.5
10	235.1

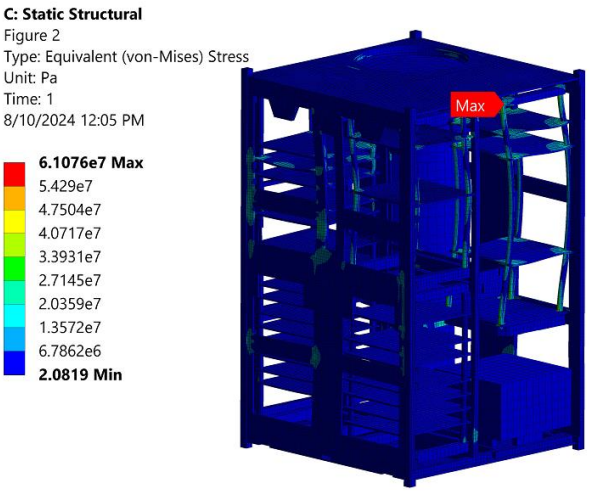

Fig. 11. Von Mises stress induced by quasi-static load.

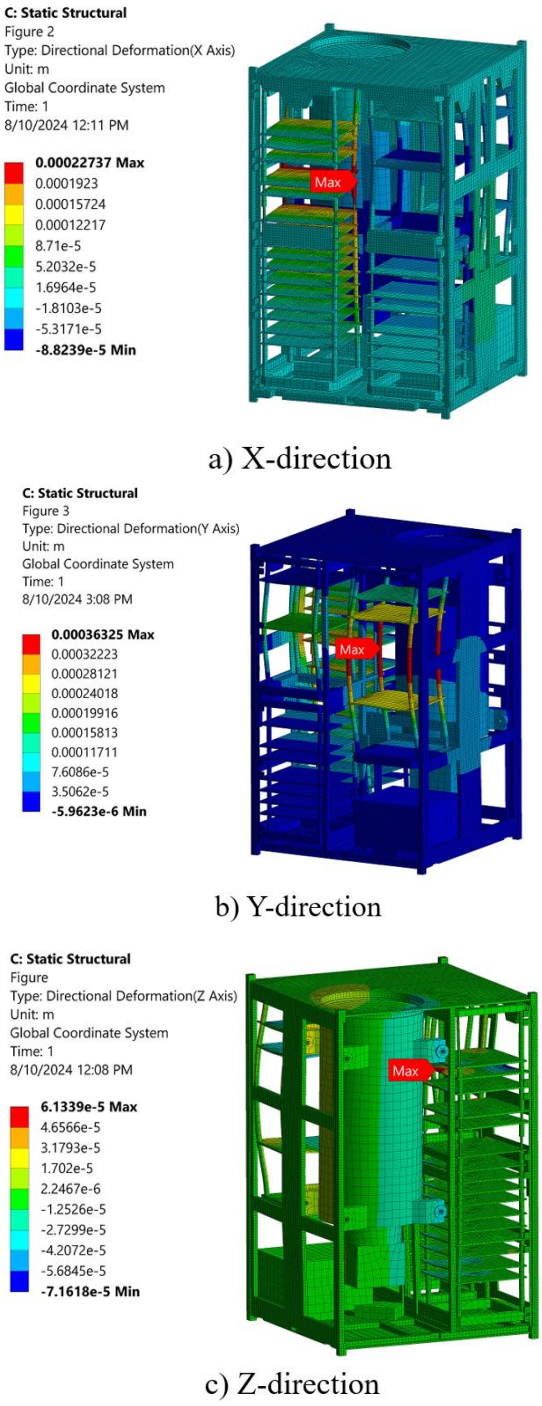

Fig. 12. Deformations induced by quasi-static load along a) X-direction (transverse), b) Y-direction (axial), and c) Z-direction (transverse)

In Figs. 13 and 14, the Von-Mises stress and deflection along the y-direction (longitudinal) induced by random vibrations are presented. In the same manner as quasi-static, the maximum stress occurred in the rod of stack 3, but with a higher magnitude of 218.4 MPA. Hence, the safety factor of the structure is equal to 2.06, which is less than

that of quasi-static, with 7.36. Also, the maximum deflection along the longitudinal direction is 0.86 mm, which is close to the allowable deflection. In Fig. 15, the power spectral density (PSD) for some critical equipment, including reaction wheels, camera, and thruster, is shown. The results show that due to the input base excitation with 4.95 g rms acceleration, the output acceleration of reaction wheels, camera, and thruster are 9.8 g, 10.3 g, and 10.1 g rms, respectively. These results are below the maximum allowable acceleration of all equipment.

In Figs. 16 and 17, longitudinal and transverse sinusoidal acceleration outputs are depicted. The results show that reaction wheels have a natural frequency of about 95 Hz along the longitudinal direction. Meanwhile, other equipment and subsystems do not have any natural frequencies below the natural frequency of the satellite. So, there need to be isolators for reaction wheels to reduce their deformations at a frequency of 94.8 Hz.

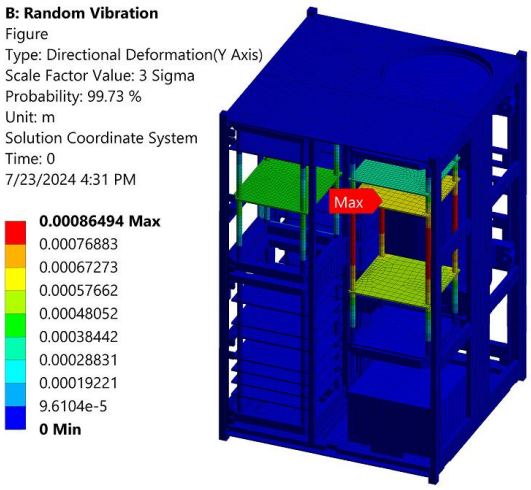

Fig. 13. Longitudinal deformations induced by random vibration

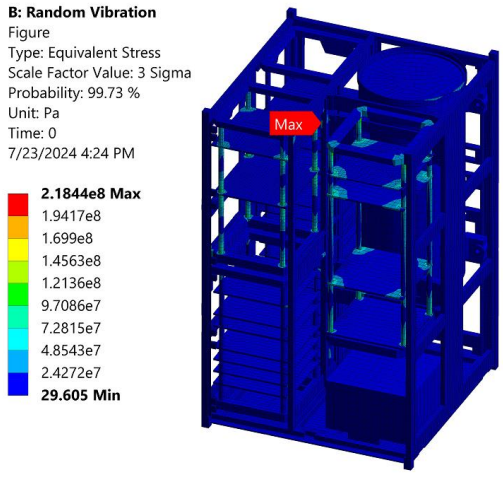

Fig. 14. Von Mises stress induced by random vibration

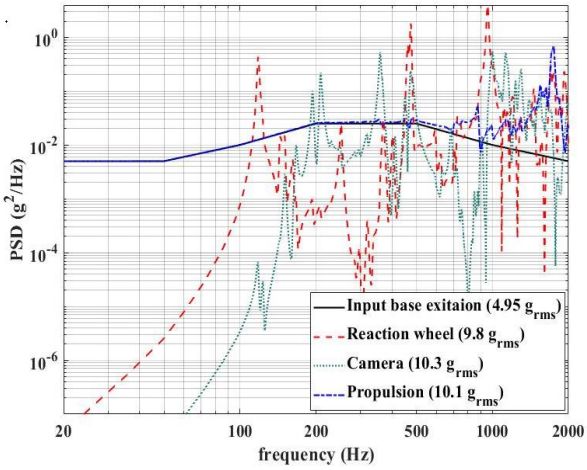

Fig. 15. Power spectral density (PSD) response for different modules, including reaction wheel, camera, and thruster

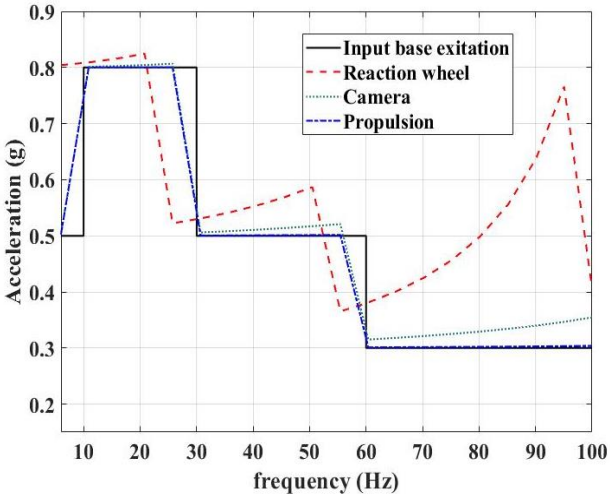

Fig. 16. Longitudinal Harmonic response for different modules, including reaction wheel, camera, and thruster

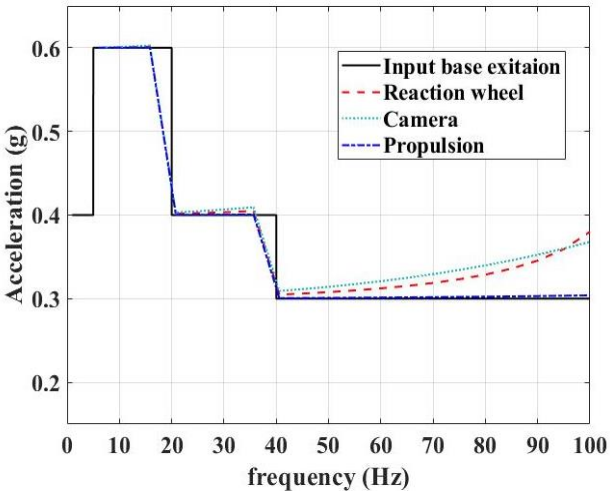

Fig. 17. Transverse Harmonic response for different modules, including reaction wheel, camera, and thruster

8 CONCLUSION

In this paper, the strength and dynamic analyses of the main structure of a 12U cubesat satellite have been performed using the finite element method. Due to the high number of available subsystems and equipment and to reduce the computational cost, except for a few cases, the lumped mass has been used for modules and equipment instead of their full models. In the strength analysis, the safety factor of the structure under quasi-static accelerations induced by the launcher during the launch phase has been 2.2. Also, due to the importance of dynamic loads during the launch of the satellite, modal analysis, random vibrations, and harmonic vibrations were conducted. The results of the modal analysis show that the first natural frequency of the satellite is equal to 118.05 Hz, which is far away from the required value by the launcher, with 65 Hz and 25 Hz along longitudinal and transverse directions, respectively. Therefore, the resonance phenomenon will not occur during the launch phase. The Von-Mises stress and deformations produced by random vibrations are 218.4 MPa and 0.86 mm, respectively, which are enough below allowable values. Also, harmonic base excitation was performed, and harmonic responses for different modules, including the reaction wheel, camera, and thruster, were calculated.

CONFLICT OF INTEREST

No potential conflict of interest was reported by the authors.

REFERENCES

[1] California Polytechnic State University. "CubeSat Design Specification". Date of visit: May 20, 2020. URL: https://www. cubesat.org/resources.

[2] A. Ampatzoglou and V. Kostopoulos, "Design, analysis, optimization, manufacturing, and testing of a 2U CubeSat, "*International Journal of Aerospace Engineering*, 9724263, 2018, https://doi.org/10.1155/2018/9724263.

[3] E. E. Bürger, G. Loureiro, R. Z. G. Bohrer, L. L. Costa, C. T. Hoffmann, D. H. Zambrano, and G. P. Jaenisch, "Development and analysis of a Brazilian CubeSat structure," *Proceedings of the 22nd International Congress of Mechanical Engineering–COBEM*, November 2013.

[4] J. E. Herrera-Arroyave, B. Bermúdez-Reyes, J. A. Ferrer-Pérez and A.vColín, "CubeSat system structural design," *In 67th International Astronautical Congress. Guadalajara, Mexico*, pp. 1-5, September 2016.

[5] G. I. Barsoum, H. H. Ibrahim, and M. A. Fawzy, "Static and random vibration analyses of a university CubeSat project," *Journal of Physics: Conference Series*, vol. 1264, no. 1, IOP Publishing, 2019, https://doi.org/10.1088/1742-6596/1264/1/012019.

[6] A. N. Alhammadi, F. Jarrar, M. Al-Shaibah, A. Almesmari, T. Vu, A. Tsoupos, and P. Marpu, "Effect of finite element model details in structural analysis of CubeSats," *CEAS Space Journal*, vol. 13, pp. 231-246, 2021, https://doi.org/10.1088/1742-6596/1264/1/012019

[7] B. Bermúdez-Reyes, J. E. Herrera Arroyave, P. Zambrano Robledo, R. Vargas-Bernal, and J. A. Ferrer Pérez, "Dynamic Computational Analysis of a Cubesat Structure to Test a New Material for a Space-Radiation Protection Shield," *In Space Fostering Latin American Societies: Developing the Latin American Continent Through Space*, Part 4, pp. 97-116, Cham: Springer Nature Switzerland, 2023, https://doi.org/10.1007/978-3-031-20675-7_6

[8] A. Ampatzoglou, A. Baltopoulos, A. Kotzakolios, and V. Kostopoulos, "Qualification of the composite structure for CubeSat picosatellites as a demonstration for small satellite elements," *International Journal of Aeronautical Science & Aerospace Research (IJASAR)*, vol.1, no. 1, pp. 1-10, 2014, dx.doi.org/10.19070/2470-4415-140001.

[9] V. M. Chau and H. B. Vo, "Structural dynamics analysis of 3-U CubeSat," *Applied Mechanics and Materials*, vol.. 894, pp. 164-170. 2019, https://doi.org/10.4028/www.scientific.net/AMM.894.164.

[10] A. Almazrouei, A. Khan, A. Almesmari, A. Albuainain, A. Bushlaibi, A. Al Mahmood and Y. Alqassab, "A complete mission concept design and analysis of the student-led cubesat project: Light-1," *Aerospace*, vol. 8, no. 9, Art. no. 247, 2021, https://doi.org/10.3390/aerospace8090247.

[11] M. Cıhan, A. Çetın, M. O. Kaya and G. İnalhan, "Design and analysis of an innovative modular cubesat structure for ITU-pSAT II," *IEEE In Proceedings of 5th International Conference on Recent Advances in Space Technologies-RAST2011*, pp. 494-499, June 2011, 10.1109/RAST.2011.5966885.

[12] V. H. L. C. Lima, R. D. N. Rodrigues, P. M. C. Lamary and R. D. A. Bezerra, "Dynamic structural analysis in a 2U CubeSat considering quasi-static loads," vol. 30, no. 1, pp. 94-108, 2022, https://doi.org/10.4067/s0718-3052022000100094.

[13] C. Güvenç, B. Topcu, and C. Tola, "Mechanical design and finite element analysis of a 3-unit

cubesat structure," *Machines. Technologies. Materials*, vol. 12, no. 5, pp. 193-196, 2018,

[14] M. R. Aswin, A. Pavithran, Y. Mangrole, and B. Ravi, "Structural and thermal analysis of a CubeSat," *In Conference of Innovative Product Design and Intelligent Manufacturing System*, pp. 363-371, Singapore: Springer Nature Singapore, November 2022, https://doi.org/10.1007/978-981-99-1665-8_32.

[15] G. N. Guentchev, M. M. Bayer, X. Li, and O. Boyraz, "Mechanical design and thermal analysis of a 12U CubeSat MTCW lidar-based optical measurement system for littoral ocean dynamics," *In CubeSats and SmallSats for Remote Sensing V*, vol. 11832, pp. 71-98, SPIE, August 2021, https://doi.org/ 10.1117/12.2597709.

[16] M. Abbasi, S. Ghazanfarinia, K. Amini, and M. Aghayi Motaaleghi, "A model-based system engineering approach for CubeSat structure and configuration management with highly constrained system design," *Engineering Solid Mechanics*, vol. 13, pp. 53-68, 2025, 10.5267/j.esm.2024.8.003.

[17] M. Hekmatfar, M. R. M. Aliha, M. S. Pishvaee, and T. Sadowski, "A robust, flexible optimization model for 3D-layout of interior equipment I a multi-floor satellite," *Mathematics*, Vol. 24, No. 11, 2023, https://doi.org/10.3390/math11244932.

[18] M. Aliha, M. Hekmatfar, M. Pishvaei, and S. Mirsaman, "Multi-Floor Equipment Layout Design in Cylindrical Satellites via Optimization Techniques," *Space Science, Technology, and Applications*, vol. 3, no. 2, 2024.

[19] C. Quiroz-Garfias, G. Silva-Navarro and H. R. Cortés. "Finite Element Analysis and Design of a CubeSat Class Picosatellite Structure," *Fourth International Conference on Electrical and Electronics Engineering (ICEEE)*, https:doi.org/10.1109/ICEEE.2007.4345026.

[20] E. E. Bürger, G. Loureiro, R.Z.G. Bohrer, L.L. Costa, C.T. Hoffmann, D.H. Zambrano, and G.P. Jaenisch, "Development and analysis of a Brazilian CubeSat structure," *Twenty-second International Congress of Mechanical Engineering (COBEM 2013)*. Ribeirão Preto, Brazil. Nov. 3-7, 2013.

[21] F. T. Al-Maliky and M. J. Albermani, "Structural analysis of KufaSat using Ansys program," *Artificial Satellites*, vol. 53, no. 1, pp. 29-35, 2018.

[22] T. Sarafin and W. F. Larson, *Spacecraft structures and mechanisms: from concept to launch*, Wiley J. Larson, 2009.

[23] "Soyuz user's manual," at the Guiana Space Centre User's Manual Issue 2, Revision0, March 2012.

HOW TO CITE THIS ARTICLE
A. R. Haddadi, S. M. Navid Ghoreishi, Y. Sedigh, and H. Shabani, "Quasi-static and Dynamic Analysis of a 12U Cubesat Under flight-phase Environmental Loads," *Journal of Aerospace Science and Technology*, Vol. 18, Issue 2, 2025, pp. 88-98.
DOI: https://doi.org/10.22034/jast.2025.475926.1207
URL: https://jast.ias.ir/article_197517.html